University of Tennessee, Knoxville
Trace: Tennessee Research and Creative Exchange

University of Tennessee Honors Thesis Projects | University of Tennessee Honors Program

Spring 5-2008

A fluorescence-based assay for eukaryotic ribonucleotide reductase I/Smll dissociation constant measurement

John Cauldet LaMacchia
University of Tennessee - Knoxville

Follow this and additional works at: https://trace.tennessee.edu/utk_chanhonoproj

Recommended Citation
LaMacchia, John Cauldet, "A fluorescence-based assay for eukaryotic ribonucleotide reductase I/Smll dissociation constant measurement" (2008). *University of Tennessee Honors Thesis Projects.*
https://trace.tennessee.edu/utk_chanhonoproj/1202

This is brought to you for free and open access by the University of Tennessee Honors Program at Trace: Tennessee Research and Creative Exchange. It has been accepted for inclusion in University of Tennessee Honors Thesis Projects by an authorized administrator of Trace: Tennessee Research and Creative Exchange. For more information, please contact trace@utk.edu.

A fluorescence-based assay for eukaryotic ribonucleotide reductase I/Sml1 dissociation constant measurement

by
John LaMacchia

Submitted to the University of Tennessee in partial fulfillment of graduation requirements for Chancellor's Honors

Department of Biochemistry and Molecular & Cellular Biology

December 2007

Abstract:

As the catalyst for the rate-limiting reaction step of *de novo* DNA synthesis, the enzyme ribonucleotide reductase (RNR) stands as an important biochemical hub within the cell. During rapid cell growth and DNA damage, an increase in RNR activity is observed that corresponds with the increased rate of DNA replication. Furthermore, inhibition of RNR in cancerous cells has shown to slow tumor growth, indicating that the enzyme is a legitimate target for anti-cancer therapy. While several drugs that function as RNR inhibitors have proven effective against certain forms of cancer, chemotherapy that targets RNR could always be improved in both efficacy and specificity (i.e. minimization of side-effects). Thus, further knowledge related to more effective means for RNR inhibition has direct clinical applications and is a topic of great research interest.

This project aims to develop and implement a fluorescence-based assay for the determination of the dissociation constants—a measure of two molecules' affinity for one another in solution—between different forms of RNR from the baker's yeast *Saccharomyces cerevisiae* (wild-type and the E689A mutant) and its natural protein inhibitor Sml1. The exact structural details of how these two proteins interact—details that could provide a valuable framework for the design of novel RNR drugs—are currently unknown, although it has been confirmed that Sml1 binds the large subunit of yeast RNR, known as Rnr1. Therefore, the assay will be designed to quantify Rnr1-Sml1 interactions, which will be measured indirectly through changes in the fluorescence anisotropy of Sml1 as the concentration of Rnr1 is increased. By comparing the differences in Sml1's binding affinity for wild-type Rnr1 versus the E689A Rnr1 mutant,

it is hoped that valuable information will be obtained about which Rnr1 residues interact with Sml1 and are involved in its binding.

Background:

Ribonucleotide reductase (RNR) is an enzyme found in all organisms and is responsible for catalyzing the conversion of ribonucleosides—UDP, CDP, GDP, and ADP—to 2'-deoxyribonucleoside diphosphates[1] (2'-deoxy-TDP is synthesized by thymidilate synthase[2]). As such, RNR is responsible for maintaining the proper balance of cellular dNTP pools, which must be finely tuned to insure that DNA replication takes place in a timely and accurate manner. If dNTP pools are too low, replication rates decrease; if too high, mutation rates of vital genes increase. Either way, the ultimate result is cell death. Thus, RNR is regulated extensively, both at the transcriptional[3] and allosteric[4] levels, as well as through subcellular localization in eukaryotes. [5] Due to human RNR's status as a target for effective anti-cancer treatment via drugs such as hydroxyurea[6,7] and Gemcitabine[8], which interfere with RNR activity, there has been much interest in the molecular/structural basis of RNR catalysis and inhibition, as well as in the structural details of RNR's interactions with these drugs.[9] More recently, considerable research has been devoted to the development of peptidomimetic-based RNR inhibitors (molecular mimics of short peptides) that bind the enzyme with high specificity and affinity.[10,11,12,13] Generally speaking, novel and increasingly effective mechanisms for RNR inhibition are currently highly sought after due to the great potential for clinical applications.

Mechanistically, RNR is unique among enzymes in its utilization of long-range, radical-dependent electron transport for catalysis—in fact, it was the first protein radical

discovered.[14] However, because the RNR reaction mechanism itself is so highly conserved throughout the species, different types of RNR are distinguished on the basis upon which they generate their free radical, and are divided accordingly into three main classes: I, II, and III. Class I RNR—the type found in eukaryotes—utilizes a diiron cofactor to produce a radical on one of the protein's tyrosine residues.[15,16] The major steps of the Class I reaction mechanism, as determined in *Escherichia coli* RNR, include: (1) the generation of a tyrosyl radical (Y122) on the β subunit Rnr2, (2) the transport of the electron from Rnr2 to the catalytic subunit Rnr1 via several amino acid intermediates, (3) the formation of a catalytic thiyl radical (C439) on Rnr1, and (4) the reduction of the nucleoside in the active site (involving the residues C439, C462, C225, and E441) through a 3'-keto radical intermediate.[17]

While *E. coli* RNR has provided mechanistic insight that is extendable to the human enzyme, it has also been shown that *S. cerevisiae* RNR is a good model for obtaining relevant *structural* information due to its high sequence identity (66%) and similarity (83%) with human RNR. The yeast enzyme complex exists as an $\alpha_2\beta\beta'$ hetero-oligomer in solution, with both α-subunits catalytically active. The α-subunit, or large subunit, Rnr1 (888 residues; 99.6 kDa) contains the catalytic site as well as the allosteric, effector, and specificity sites essential for proper regulation of substrate specificity. The β subunit Rnr2 (399 residues; 46.1 kDa), as mentioned above, contains the diiron radical essential for initiation of catalysis. Finally, the β' subunit Rnr4 (345 residues; 40.0 kD), which is found in *S. ceravisiae* but not *E. coli*, is thought to either provide structural support for the complex[18,19] or assist in iron binding.[20] Recently, the three-dimensional X-ray crystal structures of *S. cerevisiae* Rnr1 bound with various substrates and effectors

were solved by Xu *et al 2006.* These structures, in addition to providing a completely ordered picture of the catalytic site that was consistent with the previously proposed catalytic mechanism, also revealed another important region of the protein, Loop 2, which, by undergoing conformational shifts in an effector-dependent manner, confers RNR with the ability to preferentially bind and reduce one particular nucleoside over the others.[21]

The regulation of RNR in *S. cerevisiae*, in addition to the previously mentioned mechanisms, also involves the inhibitory action of the 12 kD (104 residue) protein *Sml1.*[22] While its exact mechanism for RNR inhibition is currently unknown, Sml1 has been shown to bind to the Rnr1 subunit in a 1:1 ratio with a dissociation constant of 0.4 uM. Also, the presence of Sml1 in a RNR solution does not affect the Rnr1 dimer/monomer equilibrium or Rnr1-Rnr2 association/dissociation equilibria, suggesting the possibility that the Rnr1 binding site for Sml1 is distinct from those for Rnr1 (dimerization), Rnr2, and Rnr4. Interestingly, while there has not been an Sml1 gene identified in mammals, yeast Sml1 nevertheless binds to and inhibits mouse Rnr1.[23] This indicates that the structural details of Rnr1-Sml1 interactions—details currently unknown due to the lack of a crystal structure of the complex—may be relevant to the development of novel human RNR inhibitors, thereby justifying investigation of the yeast Sml1-Rnr1 binding mechanism on the basis of drug design.

Often, when the three-dimensional X-ray crystal structure of a protein complex is lacking (such as is the case with the Sml1-Rnr1 pair), valuable structural information about protein-protein binding can still be obtained via less direct means. One such approach involves measuring and comparing the binding affinities, usually expressed as

dissociation constants (K_d), of various mutant binding-pairs (in which one or more known residues are altered in the protein about which structural data is desired) to the wild-type pair. Relative changes in affinity indicate that the altered residue is somehow involved—directly or indirectly—in the binding of the other protein. Therefore, by analyzing many different mutants, a picture can be built—one residue at a time—of the regions within the protein likely involved in binding.

Here, the above approach was applied to the Sml1-Rnr1 binding pair through the development and utilization of a fluorescence-based assay for the measurement of dissociation constants between Sml1 and two forms of Rnr1: wild-type (WT) and the E689A mutant. By comparison of the K_d obtained for WT Rnr1 and a previously published value (15), an effective benchmark would be provided for the assay's accuracy and precision. The E689A Rnr1 was selected for K_d measurement due to previous biochemical data that showed that the IC_{50} value (the concentration of Sml1 at which half of the activity of Rnr1 is lost) is lower in the mutant than in the wild-type. If this is the case, and if Sml1 inhibition does in fact rely on direct Rnr1 binding, then the E689A-Rnr1·Sml1 K_d should be lower than that of the WT (eg: it should bind more tightly to the mutant than to the wild type protein).

The assay was designed to be capable of screening, over short periods of time, many different Rnr1 mutants for Sml1 affinity changes, and also to provide a measurable signal that was highly specific to the actual binding event (i.e.—a signal relatively impervious to random molecular events). Essentially, the assay involved: (1) the labeling of the C14S/S60C Sml1 double mutant with a small molecule fluorescent probe: thiol-reactive Alexa C5 Maleimide 350 dye[24], (2) the titration of the labeled Sml1 solution

with Rnr1 (either wild-type or E689A mutant) with simultaneous measurement of changes in fluorescence, and (3) the generation of an Sml1-Rnr1 binding curve from which a dissociation constant could be extracted.

There are several practical reasons that Sml1 was chosen over Rnr1 to serve as the fluorescent protein. First, because this assay addresses the Sml1 binding site *on* Rnr1, not vice-versa, the affinity of multiple Rnr1 variants (here, Wt and the E689A mutant) for a single Sml1 mutant (here, the C14S/S60C double-mutant) must be analyzed. If Sml1 is labeled, then as long as the desired yield is obtained, only one reaction round is necessary. Second, for this assay, a high signal to noise ratio depends on a large change in the tumbling rate of the fluorescent protein (see next paragraph through p. 8). Because changes in tumbling rate are proportional to changes in molecular mass (as affected by a binding event), Sml1 was also selected as the fluorescent protein because its molecular weight (12 kD) is much smaller than that of Rnr1 (99.6 kD); upon binding, the effective change in MW of the fluorescent protein is thus nearly 1000%. Lastly, the C14S/S60C Sml1 mutant, because it contains a single cysteine residue, was chosen on the basis that tagging it with the thiol-reactive Alexa Fluor tag would produce only one conjugation state.

To address the issue of specificity, the measured quantity of the assay was not merely scalar fluorescence intensity, but rather fluorescence *anisotropy (r)*. A description of the degree to which a solution of fluorescent molecules, upon excitation by plane-polarized light, fluoresces in a direction parallel to the excitation beam, anisotropy is by definition a population event.[25,26] It hinges on the fact that the only fluorophores excited by plane-polarized light in a solution are those whose dipole moments—at the instant the

beam passes through the solution—are aligned with the plane of the beam. Anisotropy is best understood mathematically through the following equation, where it is defined in terms of polarized emission intensity *(I)* that is either parallel ($I\parallel$) or perpendicular ($I\perp$) to the polarized excitation beam (17, 18):

$$(Eq.\ 1)\ r = (I\parallel - I\perp)/(I\parallel + 2\,I\perp)$$

If anisotropy, in the case of freely tumbling fluorophores in solution, is conceptualized as the degree to which an excitation signal's direction vector is "randomized" by the fluorophores' random (Brownian) tumbling, then it becomes apparent why relative values of anisotropy for a given solution are proportional to relative fluorophore tumbling *rates*. In fact, anisotropy is related to the tumbling rate (specifically, the rotational correlation time, Φ) and the lifetime of the fluorophore, τ, through the Perrin equation, in which r_0 is the *limiting (maximum theoretical) anisotropy* (18):

$$(Eq.\ 2)\ r = r_0/(1 + [\tau/\Phi])$$

Because fluorescence lifetime is a kinetic parameter, its value can be assumed as constant for a given fluorophore. Thus, a change in the fluorescence anisotropy of a given solution will be directly proportional to the change in the fluorophore's rotational correlation time, which can also be expessed as a function of solution viscosity (η), temperature *(T)*, and fluorophore volume *(V)* (R equals the ideal gas constant) (18):

$$(Eq.\ 3)\ \Phi = \eta V/RT$$

For a protein, volume is proportional to the molecular mass; therefore, changes in protein mass—inherent in any protein-protein binding event—correlate directly to changes in that protein's fluorescence anisotropy according to equations 2 and 3. Here,

the measurement of changes in a fluorescence-labeled Sml1 solution's anisotropy upon incremental addition (titration) of Rnr1 provides binding data in the form of percent saturation (% bound or % unbound). This is represented by the following equation, in which r is the measured anisotropy at a given titrant (Rnr1) concentration, r_F is the anisotropy of the solution when it is completely in the unbound state (as is assumed to be the case when no Rnr1 is present), and r_B is the anisotropy of the solution when it is completely in the bound state (assumed to be equal to the maximum r observed during an Sml1/Rnr1 titration) (18):

$$(Eq.\ 4)\ \%\ Bound = (r - r_F)/(r_B - r_F)$$

Of course, if the quantum yield (Q) of the fluorescent probe changes as Sml1 transitions from bound to unbound states, then the measured anisotropy values will be weighted in favor of the state with the higher Q (*i.e.* the higher fluorescence emission intensity) and will not serve as an accurate representation of percent saturation. In this case, a correction factor must be applied to equation (above) to produce equation (below), in which (Q_B/Q_F) is the ratio of the fluorophore's quantum yields in the bound and unbound states. Here, Q_F is assumed to be equal to the fluorescence emission intensity of the Sml1 solution in the absence of Rnr1, and Q_B is assumed to be equal to that when the maximum amount of yRnr1 has been added (18):

$$(Eq.\ 5)\ \%\ Bound = (r - r_F)/[(r_B - r)(Q_B/Q_F) + (r - r_F)]$$

Materials and Methods:

Expression and Purification of S. cerevisiae Sml1 S60C Mutant:

BL21 (DE3) pLysS *Escherichia coli* cells transformed with the S60C/C14S Sml1 expression plasmid were cultured overnight at 37 deg. C in 50 mL of Luria Broth in the presence of 34 mg/L of Chloramphenicol and 100 mg/L of Ampicillin. Ten milliliters of this culture were then added to each of four 2 L flasks containing 500 mL of Terrific Broth (TB) with 34 mg/L Chloramphenicol and 100 mg/L Ampicillin. The cells were grown at 37 deg. C to an optical density (OD) of 0.6 AU measured at a wavelength of 600 nm, induced to express S60C/C14S Sml1 with the addition of isopropyl-β-D-thiogalactopyranoside (IPTG) to a final concentration of 0.5 mM, and incubated at 37 deg. C for 3 hours. They were then harvested by centrifugation at 5,000 x g (all centrifugation was performed at 4 deg. C.), resuspended in Sml1 buffer (50mM Tris pH 7.4, 10% Glycerol, 1mM EDTA, 1mM PMSF, 5mM DTT, 1x Complete protease inhibitor), flash-frozen in liquid nitrogen, and stored at -80 deg. C.

At each stage of the purification process, the presence of S60C/C14S Sml1 was confirmed by SDS-PAGE (Fig. 1). An Amersham G-75 gel filtration column was equilibrated with 150 mL of the following buffer: 50mM Tris pH 7.4, 100 mM KCl, 10% Glycerol, 1mM EDTA, 5mM DTT. The resuspended Sml1 cells were lysed by thawing at 4 deg C, and benzonase (1-3 microliters per sample) was added to degrade cellular DNA. Upon loss of viscosity, the lysate was centrifuged at 150,000 x g for 1 hour. The supernatant was collected and a 25% w/v ammonium sulfate cut was performed at 4 deg. C for 1 hour, followed by centrifugation at 12,000 x g for 30 minutes. The resulting ammonium sulfate pellet was resuspended in 2.5ml of Sml1 buffer and spun at top speed

in a Fisher Accuspin Micro tabletop centrifuge to precipitate excess ammonium sulfate. The supernatant was collected and immediately injected into the equilibrated G-75 column. S60C/C14S Sml1 was purified via size exclusion chromatography (Fig. 3). The presence of S60C/C14S Sml1 was verified by SDS-PAGE (Fig. 1), and the concentration was determined by a Bradford protein assay. DTT and excess salt were removed from the purified S60C/C14S Sml1 sample via a GE-Amersham PD-10 Desalting Column, and a Millipore Centriplus YM-10 centrifuge filter was employed to adjust the S60C Sml1 concentration to 100 μM (1.2 mg/mL).

Reaction of S60C Sml1 with Alexa Fluor C5 Maleimide Fluorophore:

Immediately following purification and concentration, the C14S/S60C Sml1 protein sample was conjugated with Invitrogen Alexa 350 Maleimide dye, according to the proprietary protocol[27] at room temperature (see "Appendix: Alexa Fluor 350 Maleimide Step-by-Step Conjugation Protocol"). In parallel, a separate control solution was prepared composed of buffer plus the same concentration of free Alexa fluor dye. These reactions were terminated after 2 hours by the addition of excess glutathione (~ 5 mg glutathione per 1 mg Alexa dye), and the C14S/S60C Sml1 containing sample was repurified via size exclusion chromatography as before (Fig. 4). This sample's buffer was then exchanged by ultrafiltration, and the presence of the Alexa fluor/S60C Sml1 conjugate (Alexa-Sml1) was verified by SDS-PAGE (Fig. 2) and a fluorescence emission scan (Fig. 4). The conjugate was then appropriately aliquoted, flash-frozen in liquid nitrogen, and stored at -80 deg. C.

Expression/Purification of Wild-Type and E689A S. cerevisiae Rnr1:

Both wild-type yeast Rnr1, which was provided by Sanath Wijerathna, as well as the E689A mutant were expressed and purified in the same manner. BL21 (DE3) pLysS cells transformed with the respective yeast Rnr1 expression plasmids were cultured overnight at 37 deg. C in 10 mL of TB containing 100 mg/L Ampicillin and 34 mg/L Chloramphenicol. The cells were then grown at 37 deg. C in (4) 2 L flasks, each containing 500 mL of the same media. When the OD at 600 nm reached 0.6 AU, the cells were chilled for 15 minutes at 4 deg. C, induced with 0.5 mM IPTG, and allowed to express yRnr1 overnight at 15 deg. C. Afterwards, the cells were harvested by centrifugation at 5000 x g for 30 min. at 4 deg. C and stored at -80 deg. C.

The cells were thawed on ice and resuspended in a lysis buffer consisting of 100 mM KCl, 50 mM HEPES-KCl pH 7.0, 5 mM $MgCl_2$, 5% (v/v) glycerol, 5 mM DTT, 1x Complete protease inhibitor, and 1 mM PMSF. Following multiple passages through French pressure at 12,000 psi, the lysate was centrifuged at 12,000 x g for 30 min. A 1.5% weight/volume streptomycin sulfate cut was then performed at 4 deg. C for 30 min., followed by 30 min. of centrifugation at 15000 x g. A 29% m/v ammonium sulfate cut was carried out on the collected supernatant, followed by centrifugation at 15,000 x g for 30 min. The supernatant was discarded and the ammonium sulfate pellet was stored at -80 deg. C.

All Rnr1 purification steps were performed at 4 deg. C. First, the ammonium sulfate pellet was thawed on ice, resuspended in buffer (50 mM HEPES-KCl pH = 7.0, 5 mM DTT, 5 mM MgCl2, 5% (v/v) glycerol, 1 mM PMSF, 1 x Complete protease inhibitor tablet), and passed through a GE-Amersham PD-10 desalting column.

Additional protease inhibitor was added and the mixture was incubated with Rnr2/Rnr4 peptide affinity resin for 1 hour. The column was washed, first with 20 mL of buffer, then with 30 mL buffer + 0.2 M KCl. Rnr1 was eluted with 10 mL of Rnr1 buffer + 1 M KCl, concentrated via ultrafiltration, frozen in liquid nitrogen, and stored at -80 deg. C.

Fluorescence Intensity and Anisotropy Measurements:

All fluorescence measurements were performed at 25 deg. C on a Perkin Elmer LS 55 Fluorescence Spectrometer coupled with Perkin Elmer FL Winlab software (Version 4.00.03). First, the Alexa-Sml1 and Rnr1 samples were thawed on ice and their concentrations were verified to 10% precision with a three-point—triplicate Bradford protein assay. The concentration of Rnr1 was then adjusted so that the desired titration increment (Wt = 60 nM; E689A = 43.7 nM) had a volume of 1 μL. Next, Alexa-Sml1 was mixed in an omnidirectional quartz fluorescence cuvette with "Rnr1 buffer" (mentioned earlier: to a final concentration of 0.50 μM. A fluorescence emission intensity scan was performed on the Alexa-Sml1 solution, using the following parameters in the 'Scan' program (single-scan mode) of Winlab: Excitation (lambda) = 346 nm; Emission range = 400-595 nm; Em./Exc. slit width = 3 nm; (lambda)/min. = 300. This was followed by a time-based intensity emission scan with the following parameters: Excitation (lambda) = 346 nm; Emission (lambda) = 440 nm; Em./Exc. slit width = 3 nm; time = 60 sec. (the fluorescence buffer emission profile was subtracted as background in both cases).

After completion of the emission scan, the "Reads" program was opened in Winlab and "Anisotropy" mode was selected. Following the calculation of G-factors, the Alexa-Sml1 solution was titrated with Rnr1 (Wt or E689A) and its fluorescence

anisotropy measured in a stepwise fashion with the following parameters: Excitation (lambda): 346 nm; emission wavelength: 440 nm; slit-widths: 3 nm; Integration Time: 30 sec. When the anisotropy appeared to have leveled off near its maximum value, one final "saturating" titration increment (containing 10x Rnr1 relative to the previous titration increments) was added and the resulting anisotropy measured. Finally, a time based intensity emission scan was performed on the saturated Alexa-Sml1/Rnr1 solution (same parameters as mentioned earlier for the "Sml1- only" solution). This entire titration was triplicated for both Wt and E689A yRnr1. Control titrations also followed this protocol, and were performed once for both Wt and E689A Rnr1 by replacing Alexa-Sml1 with an equimolar amount of Alexa-glutathione (Alexa-GSH) conjugate.

Data Analysis:

All fluorescence data (Figs. 5-9) were exported directly from FL Winlab to Microsoft Excel. Fluorescence intensity emission scan data were used to not only establish the presence of fluorescent Alexa-Sml1 (Fig. 5), but also to establish the quantum yield ratio for Alexa—Sml1 in its bound and unbound states, Q_B/Q_F (Figs. 6-7). The Alexa-glutathione "control titration" anisotropy data were treated as background noise and were subtracted from the corresponding WT Rnr1/Alexa-Sml1 and E689A Rnr1/Alexa-Sml1 measured anisotropy values. The resultant standardized values (Fig. 8) were then combined with the respective quantum yield ratios in Equation 5 (see p. 9) to obtain values for the "fraction of Sml1 bound by Rnr1" and generate binding curves for Alexa-Sml1—WtRnr1 and Alexa-Sml1—E689A-Rnr1 (Fig. 9). Finally, these binding values were exported from Excel to the Graphpad Prism data analysis suite in order to extract the respective dissociation constants. This was accomplished in "XY Graphs,"

utilizing the "One-site Binding (Hyperbola)" equation with an initial value for K_d of 0.4 μM and a constraint on maximum binding of less than 1.00. The resulting regressions (Fig. 10) and their corresponding statistical data (Table 1) were exported to and formatted in Excel.

Results/Discussion:

Initial fluorescence emission intensity scans confirmed both the presence and viability of Alexa-Sml1 (for the control runs, Alexa-GSH) as a fluorophore. The emission intensity for 0.5 μM Alexa-Sml1 at 440 nm (2.1 $x10^4$ AU) provided a relative quantum yield value for Alexa-Sml1 in the unbound state (Q_f). As increasing amounts of yRnr1 were added to the Alexa-Sml1 solution, a maximum fluorescence anisotropy value was approached, indicating that the Alexa-Sml1 was near saturation (% Bound ~ 100). The emission intensity values at 440 nm for 0.5 μM Alexa-Sml1 in the presence of 2.34 μM WT Rnr1 and 1.32 μM E689A yRnr1 provided relative quantum yield values for Alexa-Sml1 in the bound state (Q_B): 2.9 x 10^4 RU and 2.3 x 10^4 RU, respectively. These values combined with Q_F to calculate quantum yield ratios (Q_B/Q_F) for wild-type and E689A yRnr1 of 1.4 and 1.1, respectively. The fluorescence anisotropy curves (Fig. 8) provide clear qualitative indication that the E689A mutant binds C14S/S60C Sml1 more tightly than WT Rnr1.

The dissociation constant data calculated in GraphPad Prism for each titration are summarized in Table 1. For the WT Rnr1/C14S-S60C Sml1 pair, the average measured K_d equals 0.3 μM, +/- 0.09 μM, a value that falls within the error range of the previously published value of 0.4 μM, +/- 0.1 μM (15), as well as has a degree of precision similar to previously published fluorescence anisotropy data.[28,29,30] This result provides strong

indication that the assay described here is indeed a legitimate method for quantification of Rnr1/Sml1 binding. For the E689A Rnr1/C14S-S60C Sml1 pair, the average measured K_d of 0.1 μM, +/- 0.04 μM, provides evidence that Sml1 binds this mutant more tightly than wild-type, an observation that is in agreement with previous biochemical data of heightened E689A inhibition by Sml1. For both Rnr1 variants, the statistical range of the individual K_d values was less than 25% of the average value. R^2 values ranged from 0.83 to 0.85 for WT Rnr1/C14S-S60C Sml1 and from 0.85 to 0.87 for E689A Rnr1/C14S-S60C Sml1.

When considering the application of this fluorescence assay, as described, to other Rnr1 mutants for further characterization of the Sml1/Rnr1 binding mechanism, it becomes clear that there is room for optimization. As reflected in the standard error for the K_d values obtained, there were factors that significantly limited the assay's precision. Most prominently, the Bradford protein assay, which was used to determine the initial concentrations of Sml1 and Rnr1, is only capable of 90% accuracy; the use of a more precise method for concentration measurement would likely decrease the standard error significantly. Other sources of error include: precision limitations of volume measurements (pipet calibration, etc.), calibration of the data acquisition setup (spectrometer optics, etc.), and the inclusion of a limited number of data points in each binding curve (an increase in the number of titration increments from a few dozen to a few hundred would provide further refinement). In the future, minimization of these variables in this assay—perhaps through the incorporation of automated, high-throughput methods—could allow for the measurement of dissociation constant values to two significant figures. This would provide the precision necessary for detection of the small

changes in affinity from Rnr1 mutant to mutant that could be crucial to a true understanding of what is taking place structurally.

In conclusion, this fluorescence-based method provides a viable template for characterization of the Sml1/Rnr1 binding mechanism through the relative binding affinities of Rnr1 mutants. Sml1's heightened binding of the E689A Rnr1 mutant is one piece of the "mechanistic puzzle", but many other Rnr1 residues need to be addressed before a picture of how these two proteins interact structurally can begin to emerge.

Figures/Data:

Figure 1: *15% SDS-PAGE Gel of C14S/S60C Sml1 Purification. Lanes, from left to right: (1) Bio-Rad Low Range SDS-PAGE Molecular Markers, (2) Sml1 cell lysate, (3) Sml1 post-ammonium sulfate cut, (3) Sml1 supernatant post-tabletop centrifugation, (5) Sml1 after G75 size-exclusion purification (before conjugation with Alexa Fluor 350 C5 Maleimide).* <u>*Disregard lane 4.*</u>

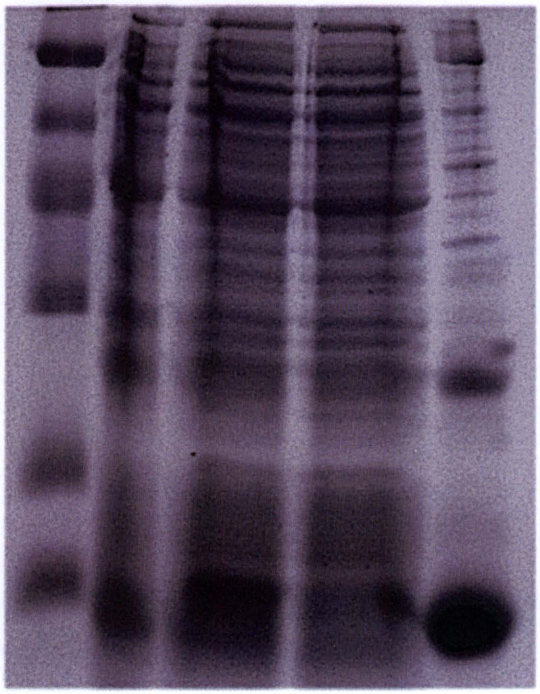

Figure 2: *15% SDS-PAGE Gel of Alexa-tagged C14S/S60C Sml1 and Wt yRnr1.*
Lanes, from left to right: (1) Bio-Rad Low Range SDS-PAGE Molecular Markers, (2,3) ***disregard****, (4) C14S/S60C Sml1 after conjugation with Alexa Fluor 350 C5 Maleimide and second size-exclusion purification, (5) Wt yRnr1 after P7-peptide affinity chromatography and concentration.*

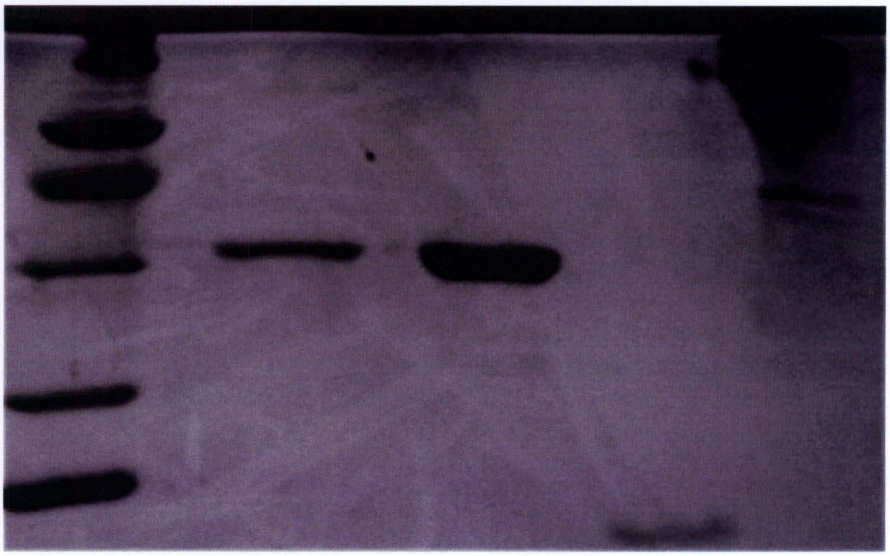

Figure 3: *Size-exclusion chromatogram of Sml1 (third peak to the right) after G75 size-exclusion purification (before conjugation with Alexa Fluor 350 C5 Maleimide).*

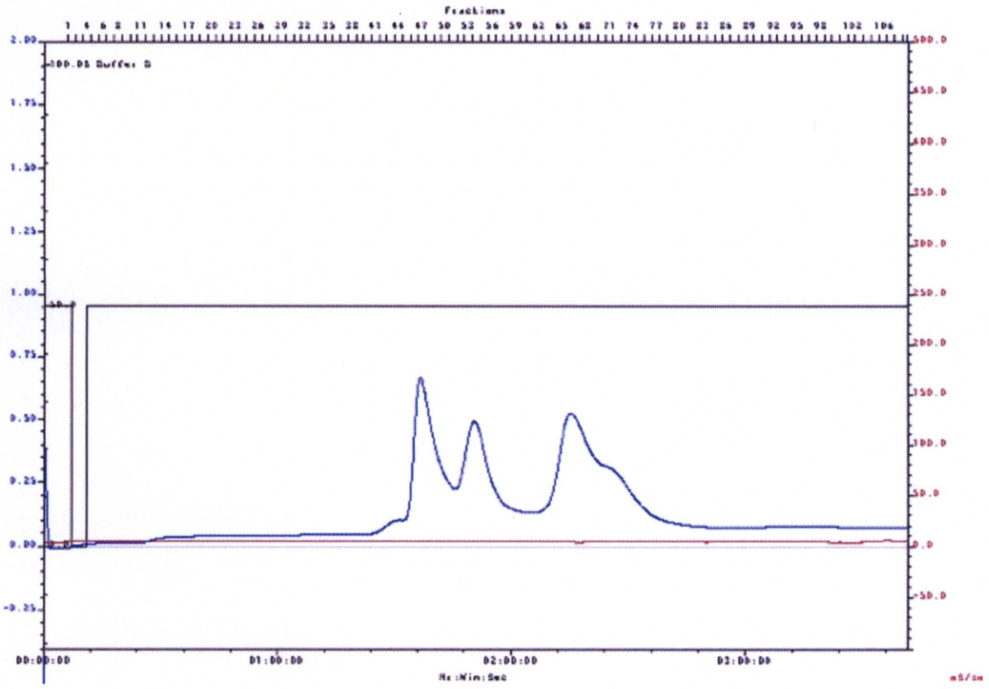

Figure 4: *Size exclusion chromatogram of C14S/S60C Sml1 after conjugation with Alexa Fluor 350 C5 Maleimide and second size-exclusion purification.*

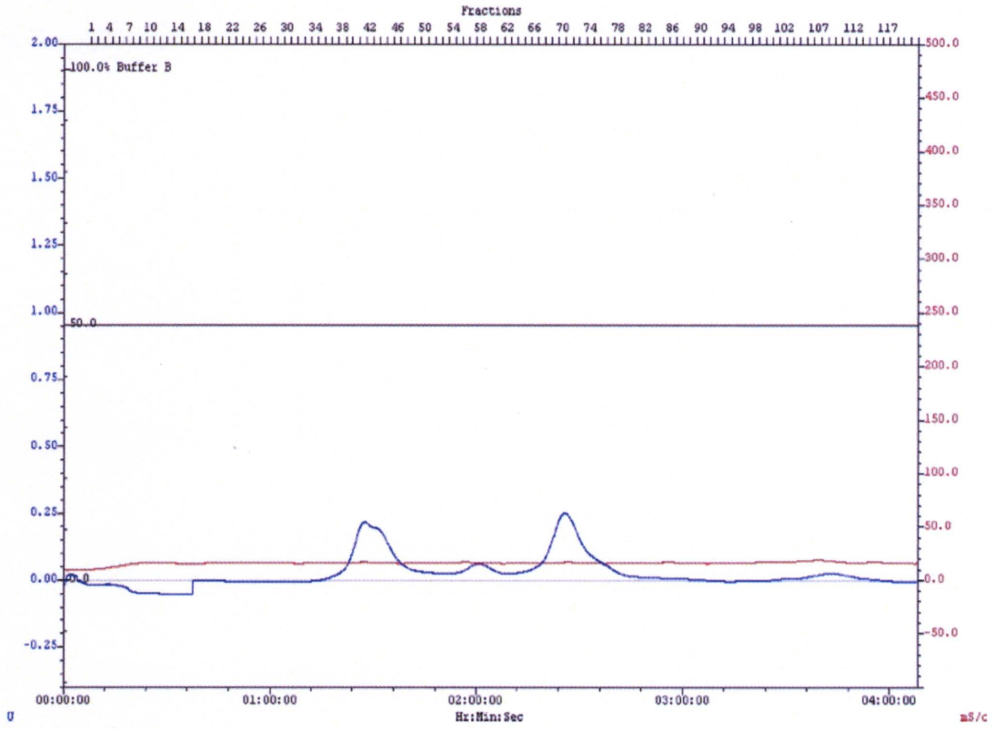

Figure 5

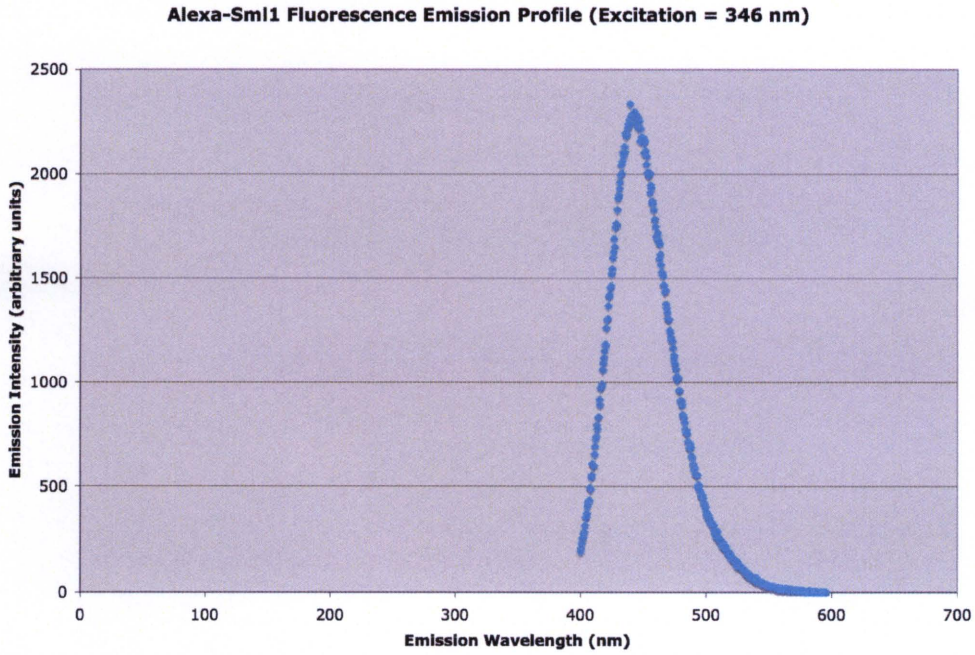

Figure 6

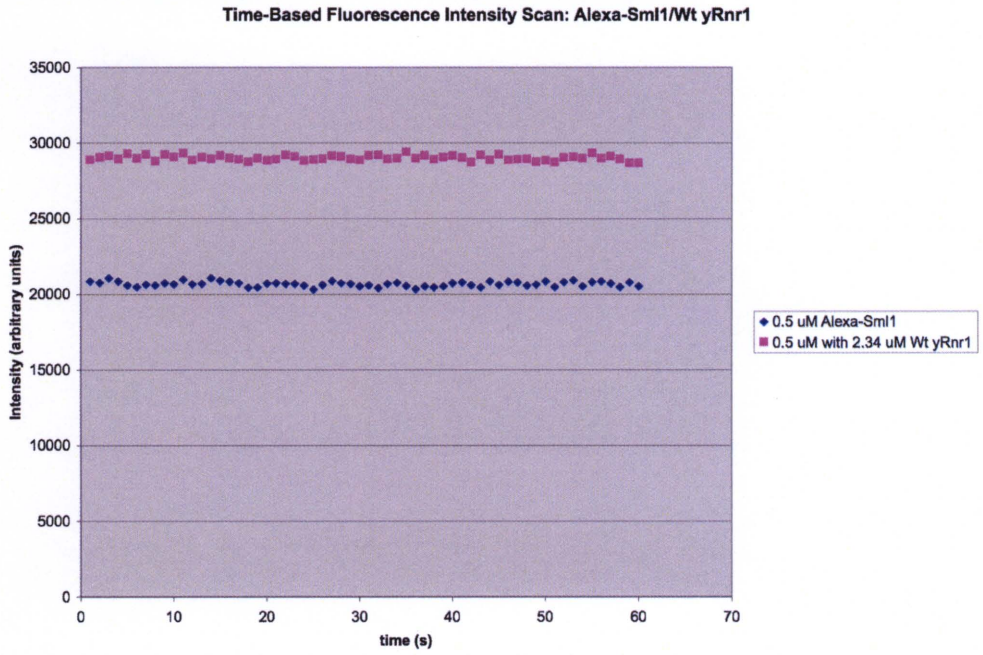

Figure 7

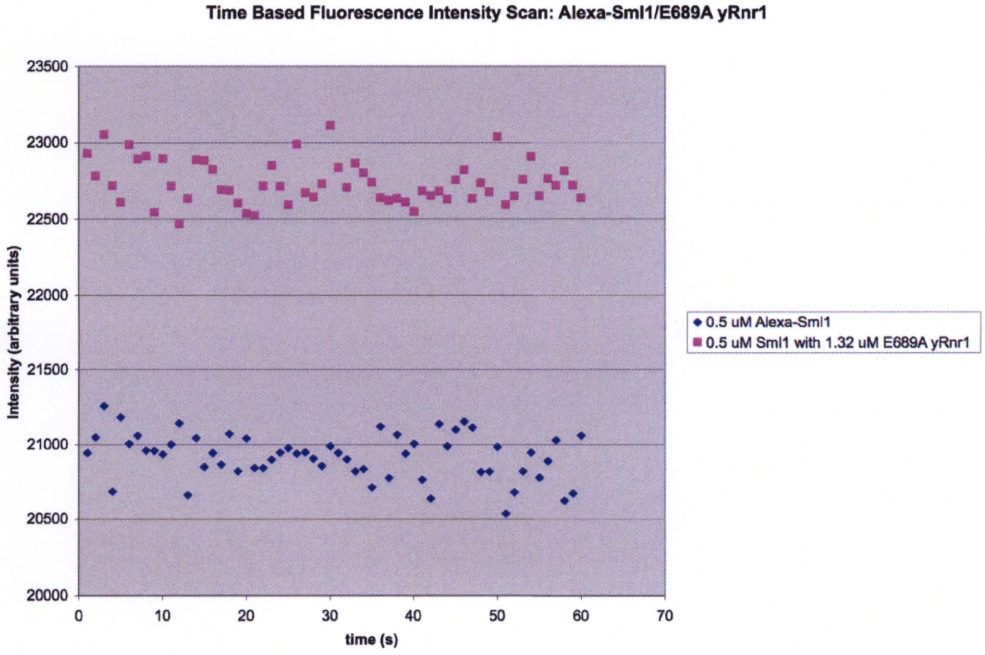

Figure 8

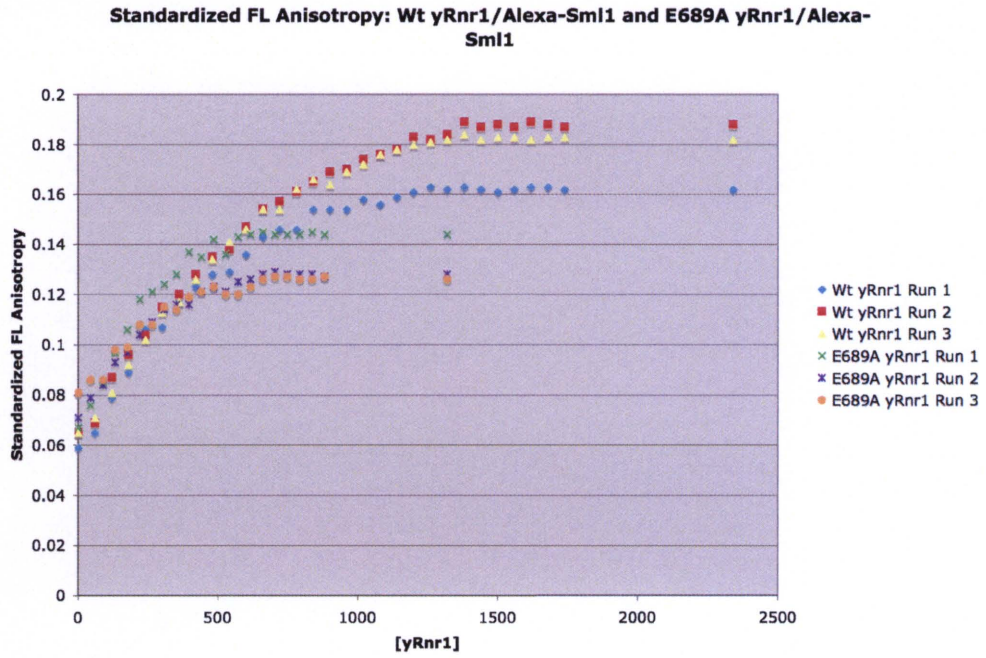

Figure 9

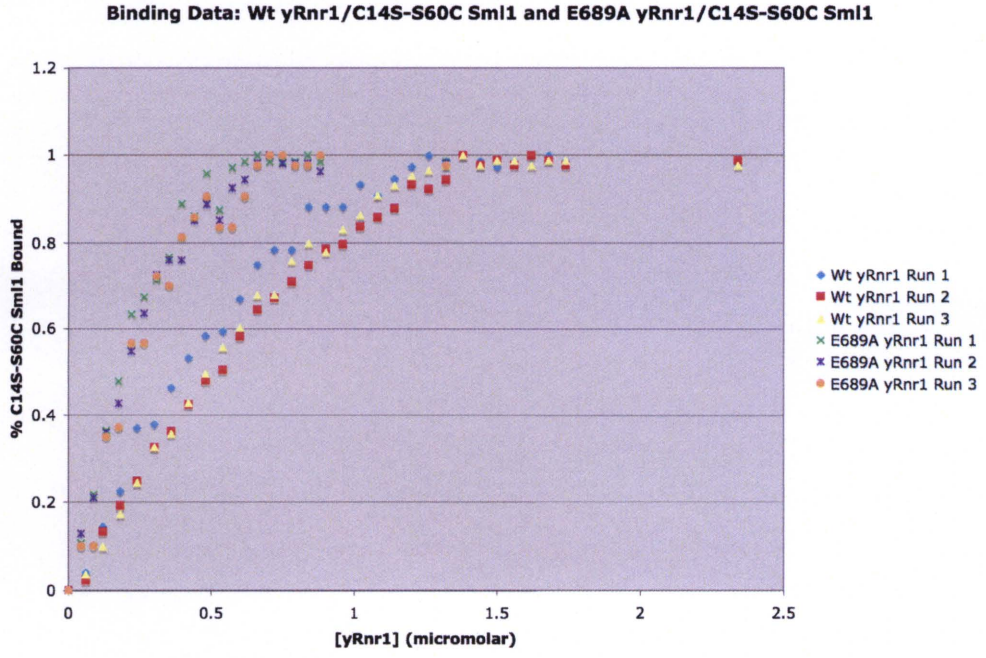

Figure 10

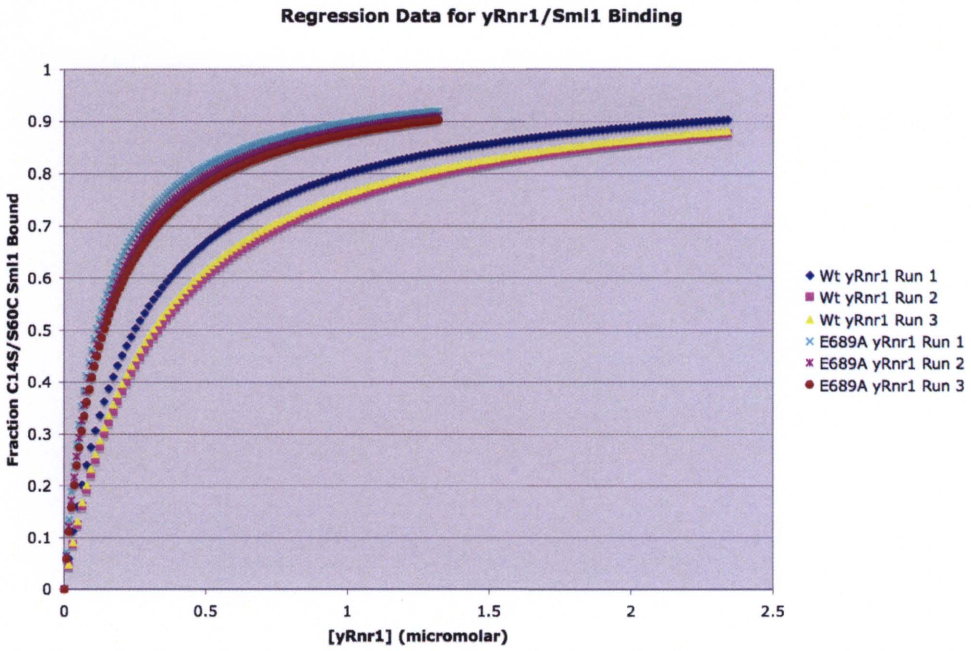

TABLE 1: Regression Statistical Data

	C14S-S60C Sml1/Wt yRnr1 Regression Analysis			Average	Kd Range/Avg. Kd	C14S-S60C Sml1/E689A yRnr1 Regression Analysis			Average	Kd Range/Avg. Kd
	Run 1	*Run 2*	*Run 3*			*Run 1*	*Run 2*	*Run 3*		
Equation: One site binding (hyperbola)										
Best-fit values										
BMAX	1	1	1	1		1	1	1	1	
KD	0.2476	0.33	0.3107	0.2961	0.278284363	0.1134	0.1287	0.1411	0.12773333	0.216858038
Std. Error										
BMAX	0.06783	0.08469	0.08636	0.07962667		0.07368	0.07278	0.08877	0.07841	
KD	0.0708	0.1012	0.1003	0.09076667		0.03771	0.03951	0.05033	0.04251667	
95% Confidence Intervals										
BMAX	0.8613 to 1.000	0.8268 to 1.000	0.8234 to 1.000			0.8463 to 1.000	0.8482 to 1.000	0.8148 to 1.000		
KD	0.1028 to 0.3923	0.1229 to 0.5370	0.1055 to 0.5159			0.03475 to 0.1921	0.04630 to 0.2111	0.03616 to 0.2461		
Goodness of Fit										
Degrees of Freedom	29	29	29	29		20	20	20	20	
R^2	0.8492	0.8433	0.8307	0.84106667		0.8577	0.8744	0.8469	0.85966667	
Absolute Sum of Squares	0.4441	0.4806	0.5416	0.48876667		0.2992	0.2534	0.3383	0.29696667	
Sy.x	0.1237	0.1287	0.1367	0.1297		0.1223	0.1126	0.1301	0.12166667	
Constraints										
BMAX	BMAX < 1.000	BMAX < 1.000	BMAX < 1.000			BMAX < 1.000	BMAX < 1.000	BMAX < 1.000		
KD	KD > 0.0	KD > 0.0	KD > 0.0			KD > 0.0	KD > 0.0	KD > 0.0		
Data										
Number of X values	31	31	31	31		22	22	22	22	
Number of Y replicates	1	1	1	1		1	1	1	1	
Total number of values	31	31	31	31		22	22	22	22	
Number of missing values	0	0	0	0		0	0	0	0	

Appendix: Alexa Fluor Maleimide Step-by-Step Conjugation Protocol

Note: *Care must be taken to protect Alexa fluorophore from light as much as possible before and during conjugation.*

1. Immediately prior to use, prepare 1-10 mM stock solution of Alexa Fluor Maleimide by dissolving in appopriate volume of DMSO.
2. Adjust protein (Sml1) concentration to 50-100 μM in suitable buffer (50mM Tris pH 7.4, 100 mM KCl, 10% Glycerol, 1mM EDTA, *without* DTT) at room temperature.
3. Place the Sml1 solution in a Falcon tube and stir. Add Alexa Fluor Maleimide/DMSO solution (10 moles Alexa fluor per mole Sml1) dropwise. Cap the Falcon tube and allow the reaction to proceed while stirring for 2 hours.
4. After 2 hours, terminate the reaction by adding an excess amount of glutathione.

Special Thanks

Copious amounts of thanks are owed by the author to many people for making this work possible: to Chris Dealwis for his continual support, guidance, and mentorship; to Joseph Racca for the grand introduction into a wonderful world of scientific discovery; to Jim Fairman and Sanath Wijerathna for the many hours of excellent training; to Brad Bennett, Richard Simmerman, and Anna Gardberg for the countless engaging and useful discussions; to Kathleen Pridgen for four years of concatenation, collaboration, commiseration; to Sid Desai and Lauren McGee for valuable discussion; to the entire Fernandez lab for bench and freezer space; finally, to Royce Nicholas Dansby-Sparks and

the University of Tennessee Department of Chemistry for fluorescence spectrometer usage.

References:

[1] Brown, N. C. & Reichard, P. (1969) *J. Mol . Biol .* **46,** 39 –55.

[2] NCBI Entrez Gene: *TYMS thymidylate synthetase [Homo sapiens]* <http://www.ncbi.nlm.nih.gov/sites/entrez?Db=gene&Cmd=ShowDetailView&TermToSearch=7298> Accessed on 10/20/07.

[3] Huang, M., Zhou, Z. & Elledge, S. J. (1998) *Cell* **94,** 595– 605.

[4] Larsson, K. M., Jordan, A., Eliasson, R., Reichard, P., Logan, D. T. & Nordlund, P. (2004) *Nat. Struct. Mol. Biol.* **11,** 1142–1149.

[5] Yao, R., Zhang, Z., An, X., Bucci, B., Perlstein, D. L., Stubbe, J. & Huang, M. (2003) *PNAS, USA.* **100,** 6628 – 6633.

[6] Elford, H.L. (1968) *Biochem Biophys Res Commun.* **33(1),** 129-135.

[7] Krakoff, I.H., Brown, N.C., and Reichard, P. (1968) *Cancer Research.* **28,** 1559-1565.

[8] Wang, J., Lohman, G., and Stubbe, J. (2007) *PNAS USA.* **104,** 14324 –14329.

[9] Xu, H., Faber, C., Uchiki, T., Racca, J., & Dealwis, C. **(2006).** *PNAS*, USA. **103,** 4028-4033.

[10] Cohen EA, Gaudreau P, Brazeau P, Langelier Y. 9 (1986) *Nature.* **321,** 441–3.

[11] Dutia BM, Frame MC, Subak-Sharpe JH, Clark WN, Marsden HS. (1986) *Nature.* **321,** 439–41.

[12] Cooperman, B.S., Gao, Y., Tan, C., Kashlan, O.B., Kaur, J. (2005) *Advan. Enzyme Regul.* **45,** 112–125.

[13] Smith, A.B., Sasho, S., Barwis, B.A., Sprengeler, P., Barbosa, J., Hirschmann, R., and Cooperman, B.S. (1998) *Bioorganic & Medicinal Chemistry Letters.* **8,** 3133-3136.

[14] Stubbe J. 1989. *Annu. Rev. Biochem.* **58,** 257–85.

[15] Sjoberg, B. M., Reichard, P., Graslund, A. and Ehrenberg, A. (1978) *J. Biol. Chem.* **253,** 6863-6865.

[16] Ehrenberg, A., Reichard, P., (1972) *J. Biol. Chem.* **247,** 3485-3488.

[17] Stubbe, J., Van der Donk, W.A. (1998) *Chem. Rev.,* **98** (2), 705 -762.

[18] Chabes, A., Domkin, V., Larsson, G., Liu, A., Graslund, A., Wijmenga, S. & Thelander, L. (2000) *PNAS, USA.* **97,** 2474 –2479.

[19] Sommerhalter, M., Voegtli, W.C., Perlstein, D.L., Ge, J., Stubbe, J., and Rosenzweig, A.C. (2004) *Biochemistry.* **43,** 7736-7742.

[20] Ge, J., Perlstein, D.L., Nguyen, H., Bar, G., Griffin R.G., and Stubbe, J. (2001) *PNAS, USA.* **98.** 10067–10072.

[21] Xu, H., Faber, C., Uchiki, T., Fairman, J., Racca, J., and Dealwis, D. (2006) *PNAS, USA.* **103.** 4022– 4027.

[22] Zhao, X., Muller, E. G., and Rothstein, R. (1998) *Mol. Cell.* **2,** 329 –340.

[23] Chabes, A., Domkin, V., Thelander, L. (1999) *J. Biol. Chem.* **274.** 36679 –36683.

[24] Obtained from Molecular Probes (Invitrogen).

[25] Ladokhin, Alexey S. *Fluorescence Spectroscopy in Peptide and Protein Analysis,* in Encyclopedia of Analytical Chemistry (R.A. Meyers, Ed.), pp. 5762 – 5779. John Wiley & Sons Ltd, Chichester, 2000.

[26] Lundblad, J.R., Laurance, M., and Goodman, R. H. (1996) *Mol. Endocrinology.* **10.** 607-612.

[27] *Thiol-reactive probes* (PDF document), Molecular Probes (Invitrogen), 2006.

[28] Sakaguchi, K., Saito, S., Higashimoto, Y., Roy, S., Anderson, C.W., and Appella, E. (2000) *J. Biol Chem.* **275.** 9278 –9283.

[29] Forwood, J.K., Harley, V., and Jans, D.A. (2001) *J. Biol. Chem.* **276.** 46575–46582.

[30] Tompa, P., Batke, J., Ovadi, J., Welch, G.R., and Sreresll, P.A. (1987) *J. Biol. Chem.* 262. **6089-6092.**